Improving Supermartensitic Stainless Steel Weld Metal Toughness

Eliminating ferrite, maximizing austenite, and softening martensite through PWHT markedly improved toughness with respect to the as-welded condition

BY S. ZAPPA, H. G. SVOBODA, N. M. RAMINI DE RISSONE, E. S. SURIAN, AND L. A. DE VEDIA

ABSTRACT

Welding of supermartensitic stainless steel plays a crucial role in fabricated components, influencing their toughness, weldability, and resistance to sulphide stress cracking. Postweld heat treatment adjusts the final properties of the weldments, bearing on microstructural evolution. The objective of this work was to maximize all-weld-metal toughness by microstructural modifications achieved by means of postweld heat treatments (PWHTs). Two all-weld-metal test coupons were prepared according to standard ANSI/AWS A5.22-95, using a 1.2-mm-diameter tubular metal-cored wire under Ar-5%He and Ar-18%CO_2 gas shielding mixtures in the flat position, with a nominal heat input of 1.6 kJ mm^{-1}. Single tempering, solution annealing, solution annealing plus single tempering, and solution annealing plus double tempering treatments were carried out at different times and temperatures. All-weld-metal chemical composition analysis, metallurgical characterization, hardness and tensile property measurements, and Charpy V tests were carried out. It was found that eliminating ferrite, maximizing austenite, and softening martensite through PWHT, improved toughness up to almost three times with respect to the as-welded condition, for both shielding gases used. When welding under Ar-18%CO_2 shielding gas, the following was detected: a) higher all-weld-metal contents of C, O, and N and slightly lower contents of Mn, Si, Cr, Ni, Mo, Cu; this fact produced slightly lower ferrite and austenite contents in the as-welded condition and b) lower toughness and ductility, and higher strength and hardness, regarding the samples welded under Ar-5%He mixture.

Introduction

Supermartensitic stainless steels (SMSS) have been developed in the last years as attractive technical alternatives to high-strength low-alloy (HSLA) steels mainly in applications related to the oil and gas industry (Refs. 1, 2). Welding of these materials plays a crucial role in fabricated components, influencing their toughness, weldability, and resistance to sulfide stress cracking. Supermartensitic stainless steels were developed based on classic martensitic stainless steels (11–14% Cr), reducing C content to enhance weldability and corrosion resistance and adding Ni to promote a free-ferrite structure and Mo (Refs. 3, 4), which also improves corrosion resistance (Refs. 5, 6).

Depending on chemical composition and welding procedure, the microstructure of SMSS deposits obtained in the as-welded condition is mainly composed of martensite with variable fractions of austenite (up to 30%) and ferrite (up to 10%), with different morphologies (Ref. 7).

Postweld heat treatment (PWHT) is usually necessary to adjust weldment properties, based on microstructural evolution. In the as-welded condition, it is common to obtain high hardness and low toughness, due to the presence of untempered martensite (Refs. 6, 8). In practice, PWHTs used involve single or double tempering treatments, promoting martensite tempering and formation of retained austenite, which results in lower hardness and higher toughness values (Refs. 4, 9). Nevertheless, these PWHTs are a considerable cost and time-consuming step in pipe welding, then in new SMSS, chemical composition has been modified to avoid PWHT or to minimize it to shorter times, less than half an hour (Ref. 10).

For welding these materials, the gas metal arc welding (GMAW) process using SMSS metal cored wires has been recognized as a suitable technological option, and its use has recently been improved (Ref. 4). This type of consumable presents several advantages such as low slag generation and high deposition rate (Ref. 11). Shielding gases employed for welding this type of material usually are inert mixes (Ar-He) or Ar-rich mixtures (Ar-CO_2, Ar-CO_2-O_2) with a very low amount of active gases (less than 5%) (Ref. 12). The type of shielding gas can affect the chemical composition of the weld metal, principally O, N, and C contents (Ref. 13).

There have been many efforts to develop tougher SMSS deposits. Control of chemical composition, particularly reducing C, O, N, and S contents or addition of Ni, has proved to be successful (Ref. 10). Besides, it is well known that the content of low toughness phases like untempered martensite or ferrite affects the final value of toughness, as well as an increased fraction of retained austenite improves it (Ref. 3). The role of precipitation reactions is not yet completely understood.

Different PWHTs lead to microstructural modifications producing different combinations of phases present in SMSS weld deposits (tempered and untempered martensite, austenite, carbides, etc.), with each microstructural pattern affecting toughness in a specific way.

S. ZAPPA (zappasebastian@hotmail.com) *is with Research Secretariat, Faculty of Engineering, University of Lomas de Zamora, Buenos Aires, Argentina. H. G. SVOBODA is with Materials and Structures Laboratory, Faculty of Engineering, Intecin, University of Buenos Aires, CONICET, Buenos Aires, Argentina. N. M. RAMINI DE RISSONE is with Deytema, Regional Faculty of San Nicolás, National Technological University, San Nicolás, Argentina. E. S. SURIAN is with Research Secretariat, Faculty of Engineering, University of Lomas de Zamora, Buenos Aires, and Deytema, Regional Faculty of San Nicolás, National Technological University, San Nicolás, Argentina. L. A. DE VEDIA is with Institute Sabato — National University of San Martín — Atomic Energy Commission, San Martín, Buenos Aires, Argentina.*

KEYWORDS

Supermartensitic Stainless Steel
Welding Procedure
Postweld Heat Treatment
Toughness

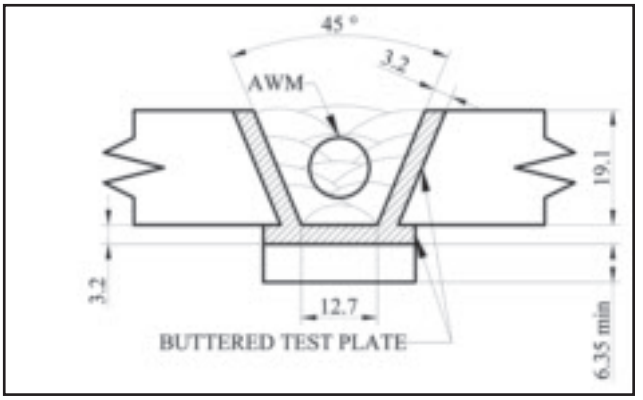

Fig. 1 — Transverse cross section for chemical analysis, microstructural characterization, and microhardness determination. (Dimensions in mm.)

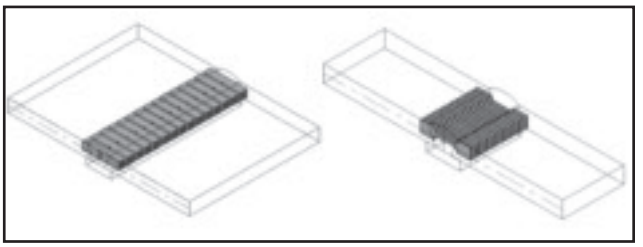

Fig. 2 — Tension test and Charpy V location.

The objective of this work was to systematically study the effect of different microstructural patterns of all-weld-metal (AWM) SMSS on toughness in order to improve this property. Additionally, the effect of interstitial elements content on toughness was evaluated, giving consideration to the shielding gas used.

Experimental Procedure

Welding

Two AWM test coupons were welded according to standard ANSI/AWS A5.22-95 (Ref. 14) using a metal cored tubular wire of 1.2 mm diameter, obtaining a SMSS weld deposit using the GMAW process with two different shielding gases. The welding parameters are presented in Table 1.

The welding position was flat; preheating and interpass temperatures were 100°C. The shielding gas flow rate was 18 L/min and the stickout 20 mm. A power source with pulsed arc of 120 Hz was employed. Both welded coupons were evaluated by radiographic testing according to ANSI B31.3 standard (Ref. 15).

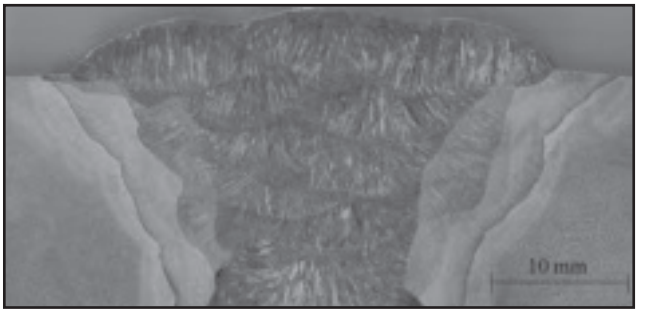

Fig. 3 — Macrography of AHaw sample.

Chemical Composition

To analyze the effect of shielding gas, transverse cross sections for chemical analysis were extracted from each coupon. AWM chemical compositions were determined by means of spectrometric measurements except C, N, O, and S contents that were analyzed via LECO™.

Postweld Heat Treatments

To induce different microstructural conditions, samples of each coupon were submitted to the different heat treatments shown in Table 2 with the corresponding sample identification.

As shown in Table 2, different PWHTs consisting of a) single tempering (650); b) solution annealing (1000); c) solution annealing plus single tempering (1000 + 650); and d) solution annealing plus double tempering (1000 + 650 + 600) were conducted maintaining as reference the as-welded condition. The PWHT parameters were selected according to previous information (Refs. 3, 8, 16) with the purpose of softening the martensite matrix, minimizing the ferrite content, and maximizing the austenite content, in order to improve AWM toughness. The overall objective was to allow the analysis and understanding of the influence of each phase present.

Single and double tempering treatments soften martensite (Ref. 17) and modify the austenite content, depending on treatment temperature and time (Refs. 8, 18). Solution annealing between 950° and 1050°C allows the dissolution of both ferrite and austenite (Ref. 18).

Microstructural Characterization

Microstructural characterization was done using light (LM), scanning electron (SEM) microscopy, and X-ray diffraction (XRD). Ferrite contents were measured following standard ASTM E562-99 (Ref. 19) by quantitative metallography and austenite contents by means of the direct peak comparison method, based on XRD patterns (Ref. 20). Dilatometric analysis has been made for AHaw and ACaw samples, to achieve a better understanding of phase transformations that take place during PWHT. Transformation temperatures A_{C1}, A_{C3}, and M_S were determined with a heating/cooling rate of 10°C/min.

Mechanical Properties

Vickers 1 kg microhardness (H_{V1}) measurements as well as Charpy V-notch (CVN) tests (Ref. 21) at 20°C were carried out for all conditions analyzed. Microhardness values were the average of at least five measurements. Charpy V-notch values were the average of at least three tested specimens. Transverse AWM tensile specimens (Ref. 22) were obtained for all conditions. All measurements were conducted in the central zone, in correspondence with the location of the notch of Charpy V specimens. Figures 1 and 2 present dimensions and locations of samples for different tests (Refs. 21, 22).

Results and Discussion

Chemical Composition

Table 3 shows the AWM chemical composition results. The values are expressed in weight percent (wt-%), except for N and O, which are in parts per million (ppm).

Samples welded under Ar-CO_2 shielding showed higher contents of C, N, and O, as well as lower contents of Mn, Si, Cr, Ni, Mo, and Cu, than those welded under Ar-He mixture.

Table 1 — Welding Parameters

Identification	Shielding Gas	Tension (V)	Current (A)	Welding Speed (mm s-1)	Heat Input (kJ mm-1)
AH	Ar-5%He	29	298	5.0	1.73
AC	Ar-18%CO_2	30	301	5.5	1.64

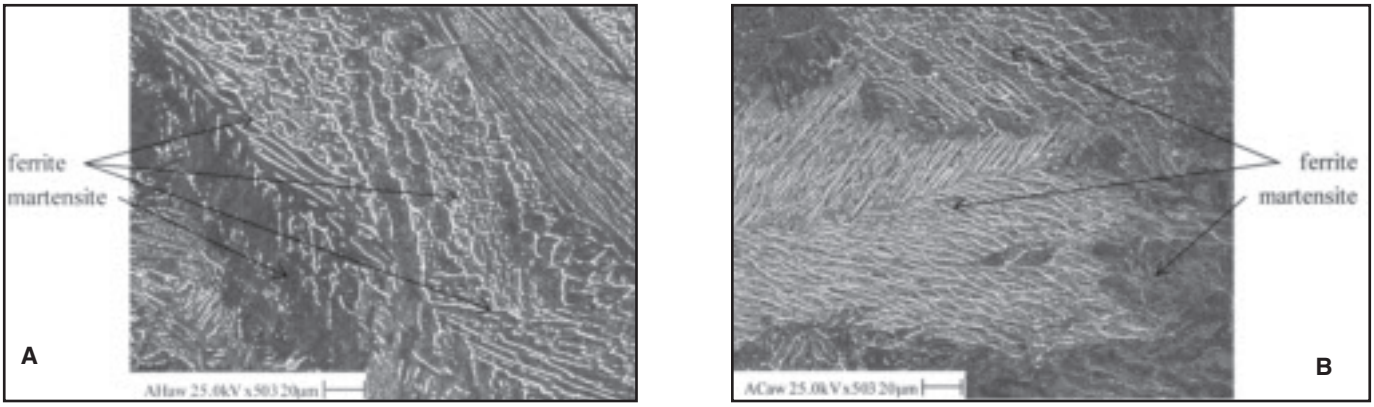

Fig. 4 — LM columnar zone microstructure of the following samples: A — AHaw; B — ACaw.

Variations observed in the metallic element contents were related to oxidation processes in the arc due to a higher oxidation potential of the shielding gas (Ref. 23). Higher contents of interstitial elements could be related to higher partial pressures of O and C in the arc atmosphere due to decomposition of CO_2 (Ref. 24).

To obtain good mechanical properties, these steels must have very low C content (0.010%) and high values of Ni (6.5%) and Mo (2.5%) (Ref. 25), together with very low levels of detrimental elements like N, O, and S (Refs. 7, 26), because they strongly affect hardness and toughness (Refs. 3, 26).

The variations observed in chemical composition could affect properties of the weld deposits. As mentioned before, C content in coupon AC (0.022%) was higher than the nominal value of 0.010% (Refs. 26, 27) reported by the consumable manufacturer; this could have led to higher hardness and lower toughness values compared to coupon AH. Coupon AC presented unexpected significantly higher O and N contents with respect to coupon AH. It has been reported that O values higher than 300 ppm, as well as a high N content, produce a strong detrimental effect on toughness (Refs. 5, 7).

It was expected that mechanical properties, metallurgical aspects, and transformation temperatures could also be affected by the observed Cr, Ni, Mo, Mn, and Cu variations. For these steels, retained austenite contents between 2 and 30% have been reported (Refs. 5, 7, 8). Ni, Cu, and Mn are known as austenite stabilizers; therefore, a higher content of these elements could increase retained austen-

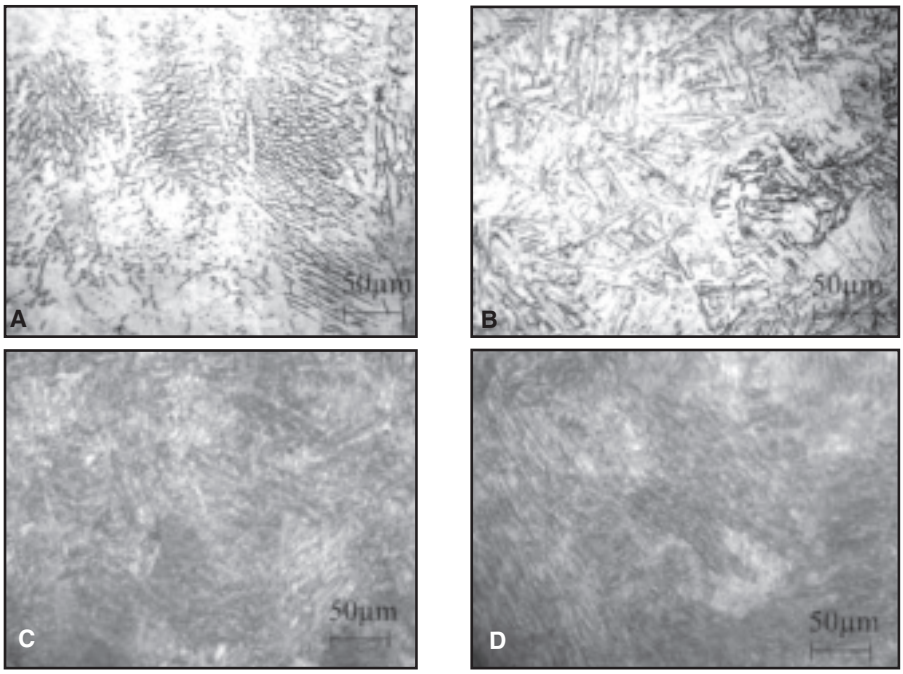

Fig. 5 — LM microstructures of samples welded under Ar-He shielding: A — AH650; B — AH1000; C — AH1000 + 650; D — AH1000 + 650 + 600.

Table 3 — AWM Chemical Composition

Element	AH	AC
C	0.012	0.022
Mn	1.76	1.61
Si	0.44	0.40
Cr	12.1	11.9
Ni	6.27	5.98
Mo	2.69	2.57
Cu	0.49	0.43
V	0.09	0.09
Nb	0.01	0.01
S	0.013	0.014
P	0.015	0.015
O (ppm)	390	610
N (ppm)	50	260

Table 2 — Identification of Samples and PWHT Parameters

Identification	PWHT Temperatures (°C)	Time (min)
AHaw	None	None
AH650	650	15
AH1000	1000	60
AH1000 + 650	1000 + 650	60 + 15
AH1000 + 650 + 600	1000 + 650 + 600	60 + 15 + 15
ACaw	None	None
AC650	650	15
AC1000	1000	60
AC1000 + 650	1000+650	60 + 15
AC1000 + 650 + 600	1000 + 650 + 600	60 + 15 + 15

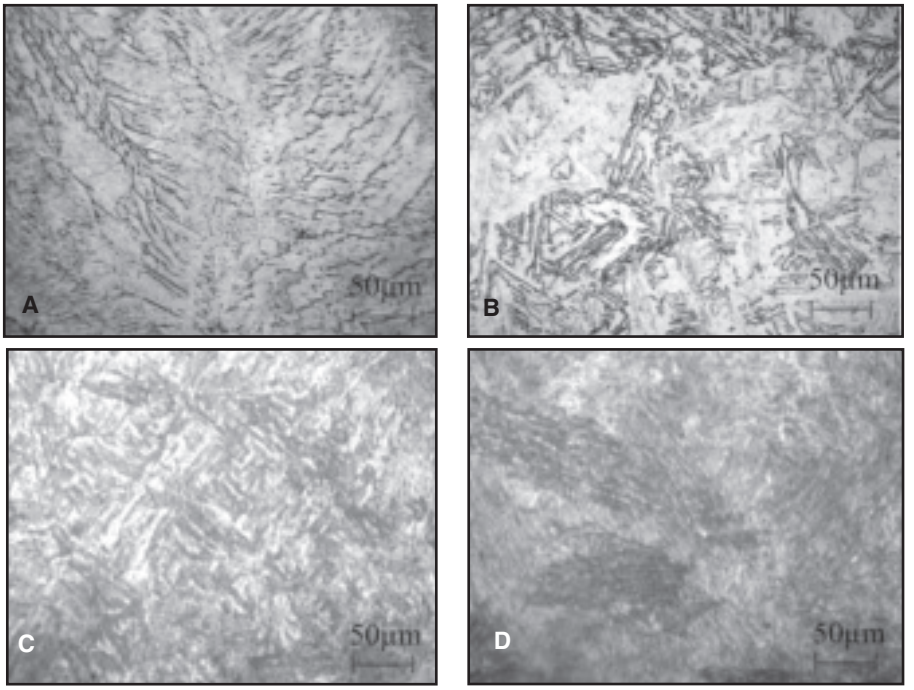

Fig. 6 — LM microstructures of samples welded under Ar-CO_2: A —AC650; B — AC1000; C — AC1000 + 650; D —AC1000 + 650 + 600.

ite percentages (Refs. 3, 8). Furthermore, Cr and Mo stabilize ferrite and a higher content of this phase is produced if these elements are increased (Refs. 3, 8).

Microstructural Characterization

Radiographic testing was evaluated with ANSI B31.3 (Ref. 15) resulting in a low level of defects. Figure 3 shows the AWM macrostructure obtained for sample AHaw.

Figure 4 shows the columnar zone microstructures for the AHaw and ACaw samples. In both cases, martensite with low fractions of ferrite was detected, as was reported previously (Refs. 1, 3, 7, 8, 12). There was no observable effect of shielding gas on the microstructure.

Two types of ferrite could be identified based on their location and morphology. Most common was ferrite with morphology similar to that of the ferrite found in duplex stainless steel weld metals. The presence of this ferrite is a consequence of incomplete ferrite-to-austenite transformation in weld metals solidifying as ferrite and was most common for more highly alloyed weld metals (Ref. 7). Another ferrite morphology, similar to that seen in austenitic stainless steel weld metals, was found in the weld metals highest in Ni solidifying as a mixture of ferrite and austenite (Ref. 7). This ferrite was located in the last solidifying interdendritic regions.

Figures 5 and 6 show microstructures for different PWHT conditions of coupons welded under Ar-He and Ar-CO_2, respectively.

There were no observable differences between the LM microstructures of both coupons for the different PWHTs. For AH650 and AC650 the microstructure did not change, showing a slight darkening associated with a precipitation phenomena. Solution annealing produced ferrite solubilization, and the microstructures that resulted were completely martensitic. Solution annealing followed by single and double tempering produced a severe darkening in the microstructure associated with carbide precipitation.

As mentioned previously, retained austenite is reported for these steels in the as-welded condition (Ref. 7). This phase was not observable by means of the microscopy techniques used in this work (Refs. 7, 8), but was detectable using the XRD technique. The XRD patterns obtained for different PWHT conditions, showing the martensite/ferrite and austenite peaks, are presented in Figs. 7, 8.

It can be seen for both as-welded samples that there was a fraction of retained austenite that diminished with the single tempering treatment and vanished after solution annealing. The single and double tempering treatments after solution annealing increased the retained austenite content, as was to be expected (Ref. 28).

Table 4 shows the results of ferrite and austenite content quantification for the analyzed conditions. Coupon AHaw showed higher contents of both ferrite and austenite than coupon ACaw.

To relate the as-welded samples' ferrite and austenite contents to the chemical composition, the expressions of Cr and Ni

Table 4 — Ferrite and Austenite Contents

Sample	Ferrite (%)	Austenite (%)
AHaw	10	20
AH650	10	15
AH1000	0	0
AH1000 + 650	0	12
AH1000 + 650 + 600	0	21
ACaw	6	18
AC650	6	7
AC1000	0	0
AC1000 + 650	0	18
AC1000 + 650 + 600	0	19

Table 5 — Cr and Ni Equivalents

Condition	Cr eq	Ni eq
AHaw	25.5	29.8
ACaw	24.6	29.5

Table 6 — Transformation Temperatures

Condition	A_{C1} (°C)	A_{C3} (°C)	M_s (°C)
AHaw	580	640	130
ACaw	640	710	125

equivalents developed by Karlsson et al. (Refs. 29, 30) for SMSS were employed in this work. Table 5 shows the results of Cr and Ni equivalents for both welding conditions. There were no significant variations in the calculated values. However, microstructure showed martensite and ferrite for the ACaw condition and martensite, ferrite and austenite for the AHaw condition, related to a higher Cr equivalent in this last sample — Fig. 9. This fact could explain the slightly higher austenite and ferrite contents measured for condition AHaw as compared to ACaw.

It was previously reported that ferrite deteriorates toughness and austenite improves this property (Ref. 31). Indeed, toughness is improved by a low-carbon soft martensite (Ref. 31). In this sense, PWHT, which minimizes ferrite, maximizes austenite, and softens martensite, could provide the best results (Ref. 31).

Martensite tempering is produced during PWHT of these steels. In general, this allows martensite softening, associated with incoherent carbide precipitation, to reach the maximum softening with the precipitation of $M_{23}C_6$ carbides at temperatures over 500°C (Ref. 32). In Ni-free alloys, PWHTs are performed at temperatures over 700°C to obtain a high reaction rate and maximum softening. Nevertheless, the presence of Ni reduces the critical temperature (A_{C1}). This temperature depends on chemical composition and heating rate, but with high Ni content it

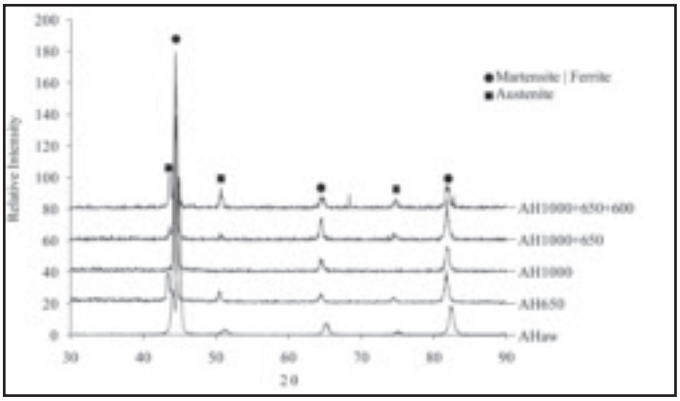

Fig. 7 — XRD patterns for samples welded under Ar-CO_2 protection, with different PWHTs.

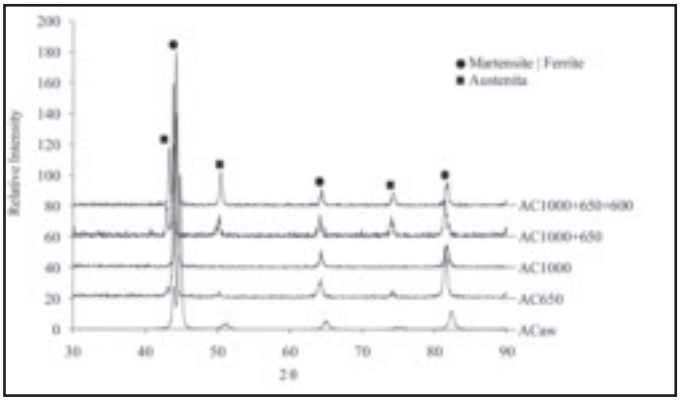

Fig. 8 — XRD patterns for samples welded under Ar-He protection, with different PWHTs.

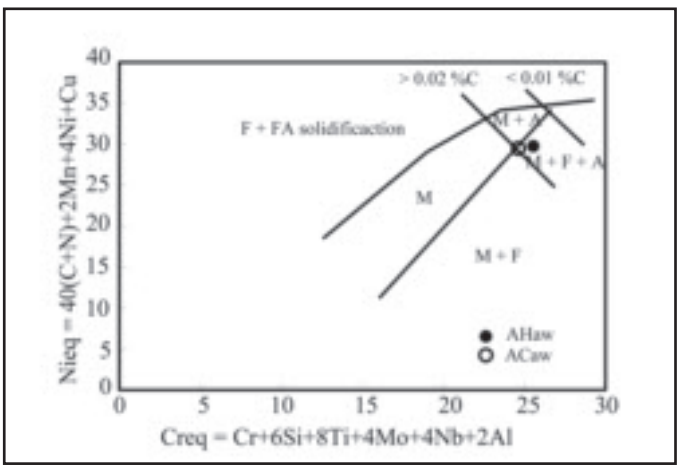

Fig. 9 — AHaw and ACaw sample locations in Karlsson et al. (Ref. 7) constitution diagram for SMSS (M: martensite; A: austenite; F: ferrite).

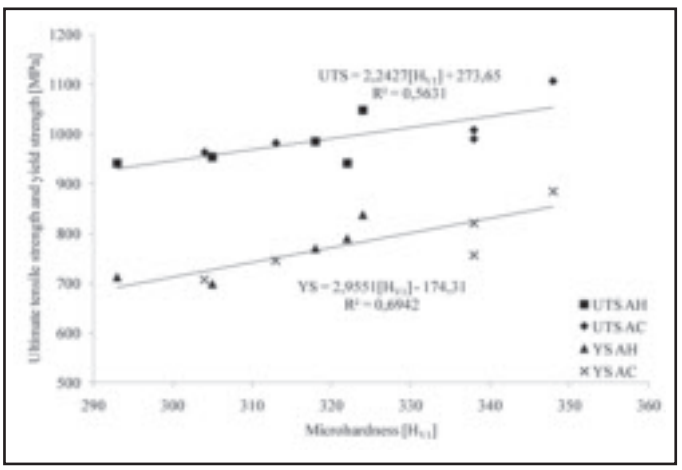

Fig. 10 — Relationship between microhardness and tensile and yield strengths.

could be as low as 500°–550°C (Ref. 32). At this temperature, the carbides' formation kinetics is very slow and under these conditions, it is normal that PWHT produces austenite for alloys 13Cr-4Ni (Ref. 32) with a different chemical composition from that of the austenite retained during welding (Refs. 32, 33). Austenite formed during PWHT will be rich in Ni, C, and Mn. The degree of enrichment will determine the stability of the austenite formed. If the PWHT is performed at temperatures slightly over A_{C1}, enriched austenite will be stable at ambient temperature. If the PWHT temperature is sufficiently higher than A_{C1}, the austenite formed will transform to untempered martensite during cooling (Ref. 32).

In Table 6, results of transformation temperature (A_{C1}, A_{C3}, and M_S) determinations for each coupon, using a heating rate of 10°C/min, can be seen. Critical temperatures (A_{C1} and A_{C3}) of the specimen ACaw were higher than those of specimen AHaw. It is known that these temperatures are heavily controlled by the chemical composition, then the changes observed could be explained in terms of the higher alloy content of coupon AHaw that produced a decrease in the transformation temperatures (Ref. 7).

In both cases, single tempering slightly reduced the austenite content, through partial transformation of austenite to martensite. Lippold and Alexandrov (Ref. 17) showed that variations of 20° to 300°C/min in heating rate produced an increase in A_{C1} of more than 100°C. A tempering heat rate of 300°C/min was used in this work. Therefore, an increased A_{C1} could be expected when tempering at 650°C, resulting in a subcritical temperature treatment. In this condition, a decrease in austenite content could be achieved.

Table 7 — Tensile Test Results

Sample	σ_{UTS}[(a)] (MPa)	$\sigma_{0.2}$[(b)] (MPa)	ε[(c)] (%)	H[(d)] (H_{V1})
AHaw	1048	838	15.7	324
AH650	941	790	17.0	322
AH1000	986	770	20.0	318
AH1000+650	954	698	27.5	305
AH1000+650+600	941	712	29.4	293
ACaw	1107	885	12.5	348
AC650	990	821	13.0	338
AC1000	1008	756	16.8	338
AC1000 + 650	982	745	17.3	313
AC1000 + 650 + 600	963	707	18.8	304

(a) — σ_{UTS}: ultimate tensile strength
(b) — $\sigma_{0.2}$: yield strength
(c) — ε: elongation
(d) — H: hardness

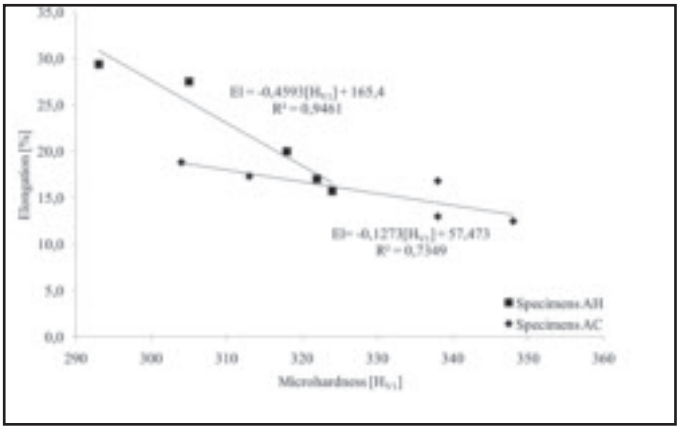

Fig. 11 — Relationship between elongation and hardness.

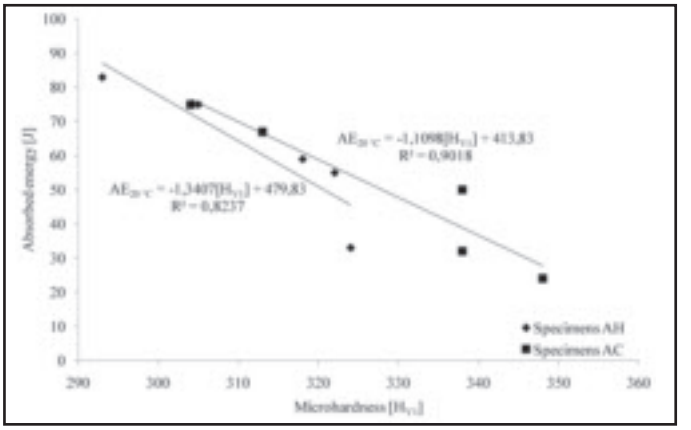

Fig. 12 — Absorbed energy at 20°C (J) vs. Vickers microhardness (HV1).

Solution annealing treatment was effective to dissolve both ferrite and retained austenite; it also produced a decrease in segregation with the matrix enrichment of the elements before being segregated (Ref. 33). The mentioned enrichment of the matrix could have generated a diminution of the A_{C1} with what the first tempering temperature after SA could have been inside the intercritical temperature zone. This fact could justify the apparition of retained austenite. Finally, the posterior treatment at 600°C (samples AH1000 + 650 + 600 and AC1000 + 650 + 600) generated a microstructure composed of tempered martensite and a higher proportion of austenite, without ferrite.

The mechanism by which the austenite content was enhanced with a double tempering could be explained by means of the thermal instabilities of austenite particles during cooling of the first tempering, according to a previous report (Ref. 3). Stability of austenite is associated with both chemical and structural factors related to a high dislocation density in the substructure. In the first tempering at 650°C (after SA), the austenite content formed during heating was increased and partially transformed to fresh martensite during cooling. At this temperature, thermal activation could have been enough to promote recovery mechanisms that allowed annihilation of dislocations, reducing the dislocation density into the austenite particles, transforming them into martensite during cooling from 650°C. After SA + 650 treatments, the microstructure was composed by tempering martensite, fresh martensite, and retained austenite. During the second tempering at 600°C (SA + 650 + 600), new austenite preferentially nucleated at the higher interfacial area recently created, and therefore, a higher amount of austenite particles were formed. It is assumed that this austenite was formed by a shear mechanism and had a high dislocation density, which did not suffer alterations at this temperature. Indeed, untempered martensite was tempered, resulting in a soft martensite matrix with uniform distributed austenite particles (Ref. 34).

Mechanical Properties

Table 7 presents hardness and tensile test results of all samples. These values were consistent with those reported previously for these types of materials (Refs. 8, 27). Higher values of hardness were detected for samples welded with CO_2 in the shielding gas. This effect could be related to higher contents of C and N in this sample, which produced a hardness increase (Ref. 3). With regard to PWHT, softening was observed in heat-treated samples. This could be related to the tempering of martensite and, in the case of sample AH, to a higher amount of austenite (Refs. 3, 35, 36). Yield and tensile strengths were slightly higher for the specimens welded under Ar-CO_2, probably associated with their higher carbon content. Figure 10 shows an approximately linear relationship between both yield and tensile strength values and hardness determinations.

Ductility was lower for specimen AC compared to sample AH. This fact could be related to the AC sample's higher values of C, N, and O, which limit ductility. Postweld heat treatment produced a reduction in strength values with a marginal improvement in ductility, as expected (Refs. 8, 18). Figure 11 presents the relationship between elongation and hardness, which showed that an increment in hardness produced a decrease in ductility. For the same hardness values, ductility in the AH samples was higher than in the AC ones. This could be related to the higher content of interstitial elements in these samples.

Table 8 presents the results obtained from Charpy V impact tests. Higher toughness was associated with lower hardness, as expected (Ref. 37). Shielding gas used during welding affected SMSS AWM toughness. With the Ar-CO_2 mixture, values of absorbed energy were lower for all the conditions studied. This fact could be associated with the higher contents of C, N, and O of samples welded under Ar-CO_2, as mentioned previously (Refs. 26, 38).

All the PWHTs improved toughness in both cases. Single tempering without SA enhanced the absorbed energy, almost duplicating the obtained values for both conditions, although the austenite fraction was reduced and there were no changes in ferrite content. This indicates that

Table 8 — Vickers Hardness and Absorbed Energy in Charpy V Impact Test

Sample	H[a] (H_{V1})	AE 20°C[b] (J)
AHaw	324	33
AH650	322	55
AH1000	318	59
AH1000 + 650	305	75
AH1000 + 650+ 600	293	83
ACaw	348	24
AC650	338	50
AC1000	338	32
AC1000 + 650	313	67
AH1000 + 650 + 600	304	75

(a) — H: Vickers hardness
(b) — E: absorbed energy in Charpy V-notch impact test at 20°C

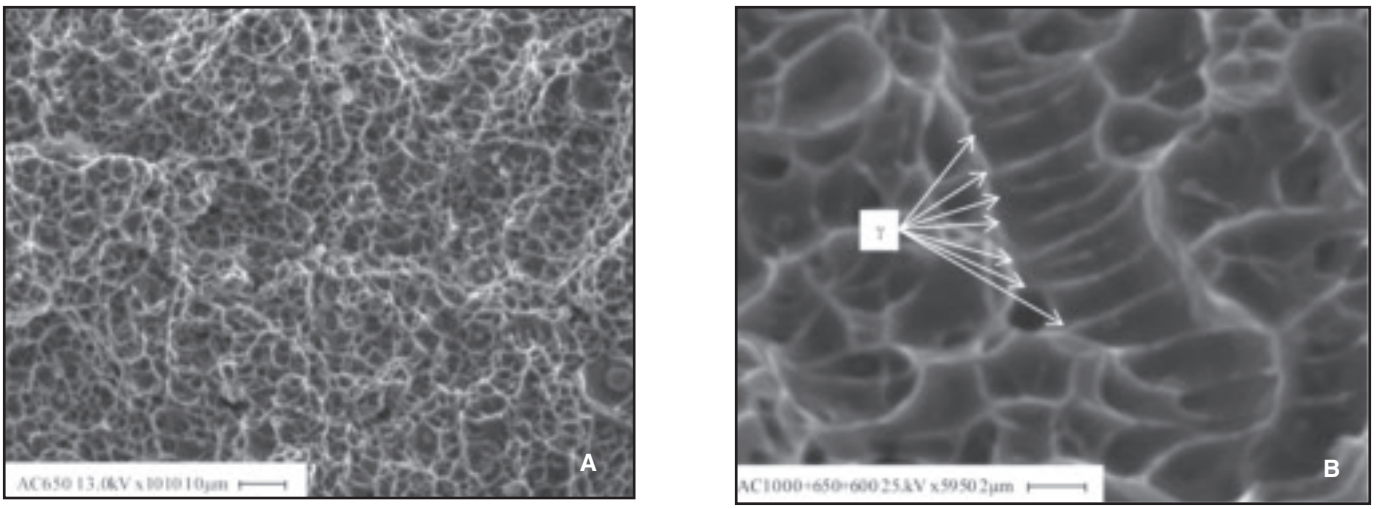

Fig. 13 — A — Fracture surface of sample AC650; B — typical dimples in the fracture surface of sample AC1000 + 650 + 600.

martensite softening was the controlling factor in this case.

Solution annealing also improved toughness for both conditions. This fact could show the effect of ferrite on this property. Some degree of martensite softening could also have occurred. For coupons welded under the Ar-He mixture, this effect was more important, consistent with the higher content of ferrite in the AW condition.

With single and double tempering after solution annealing, toughness was improved again; in this case 250 and 310% regarding the AHaw and the ACaw conditions, respectively. This could be associated with the softening of martensite, the absence of ferrite, and the finely dispersed austenite particles formed during these treatments (Ref. 39). These fine austenite precipitates promoted ductile fracture, enhancing the plastic work for fracture (Ref. 18). It was also reported (Ref. 39) that during fracture propagation in the Charpy V test, a mechanical transformation of austenite particles by localized transformation-induced plasticity mechanisms is generated, increasing the absorbed energy. Figure 12 presents the absorbed energy in Charpy V test vs. Vickers hardness. For both conditions, AH and AC, it was observed that as hardness increased, toughness decreased. However, a displacement of the AC curve to the right was observed. This effect could be related to the AC sample's higher O content, which produced a decrease in toughness according to what was previously reported for this type of material (Refs. 5, 30).

Regarding the fracture mode, it is worth mentioning that all specimens tested at room temperature displayed 100% of fibrous fracture with typical dimples and without cleavage. Figure 13A is representative of the fracture surfaces seen, this one from the AC650 sample. This typical dimple appearance showed a ductile-dimple fracture associated with a high microvoid density. This may be attributed to the existence of a large number of internal interfaces due to both nonmetallic inclusions and austenite and/or transformed austenite particles, which may act as void nucleation sites, according to previous reports for similar materials (Ref. 28). Figure 13B shows typical dimples with austenite and/or transformed austenite small particles (Ref. 28).

Conclusions

- Eliminating ferrite, maximizing austenite, and softening martensite in SMSS weld metal improved toughness up to almost three times with respect to the AW condition, for both shielding gases used. The mechanisms that explained this toughness improvement were discussed.
- When Ar-18%CO_2 shielding gas was employed instead of Ar-5%He shielding gas, higher contents of C, O, and N and slightly lower contents of Mn, Si, Cr, Ni, Mo, and Cu were detected. This variation in chemical composition produced slightly lower ferrite and austenite contents in the as-welded condition. Lower toughness and ductility, and higher strength and hardness were obtained when this shielding gas mixture was employed.
- Further studies are necessary to associate the heating rate during the PWHT, the critical temperatures of transformation, and PWHT temperatures with the stability of austenite.

The present work contributes to the better comprehension of the mechanisms involved in the toughness control of SMSS deposits, considering the effects of microstructure and some aspects of the welding procedure.

Acknowledgments

The authors wish to express their gratitude to ESAB-Sweden for the donation of the consumable and for LECO chemical analysis; Conarco-ESAB-Argentina for performing chemical analysis; Air Liquide Argentina for donating gases for welding; Latin American Welding Foundation, Argentina, for facilities for welding and mechanical testing; Scanning Electron Microscopy Laboratory of INTI-Mecánica, Argentina, for facilities for SEM analysis; and APUEMFI, Argentina and ANPCyT, Argentina, for financial support.

References

1. Marshall, A. W., and Farrar, J. C. M. 1998. Welding of ferritic and martensitic 13%Cr steels. Preliminary report (draft 2). IIW Doc IX-H-422-98: 1 to 18.

2. Farrar, J. C., and Marshall, A. W. 1998. Supermartensitic stainless steel — overview and weldability. IIW Doc No. IX-H 423-98: 1–3.

3. Bilmes, P. D. 2000. Role of austentite on mechanical properties of soft martensitic stainless steel weld metals. PhD dissertation. La Plata, Argentina. Universidad Nacional de La Plata, Facultad de Ingeniería.

4. Lippold, J. C., and Kotecki, D. J. 2005. *Welding Metallurgy and Weldability of Stainless Steels.* John Wiley & Sons, Inc.

5. Karlsson, L., Rigdal, S., Sweden, G., Bruins, W., and Goldschmitz, M. 1999. Development of matching composition supermartensitic stainless steel welding consumables. *Svetsaren* No. 3: 3–7.

6. Kvaale, P. E., and Olsen, S. 1999. Experience with supermartensitic stainless steels in flowline applications. *Stainless Steel Word*. The Hague, The Netherlands.

7. Karlsson, L., Bruins, W., Gillenius, C., Rigdal, S., and Goldschmitz, M. 1999. Matching composition supermartensitic stainless steel welding consumables. *Supermartensitic Stainless Steels '99.* Brussels, Belgium.

8. Zappa, S., Svoboda, H., Ramini de Ris-

sone, M., Surian, E., and de Vedia, L. 2007. Effect of post weld heat treament on the properties of a supermartensitic stainless steel deposited with tubular metal-cored wire. *Soldagem & Inspecão* 12(2): 115–123.

9. Bilmes, P. D., Llorente, C. L., and Solari, M. 1998. Effect of postweld heat treatment on the microstructure and mechanical behavior of 13Cr-4NiMoL and 13Cr-6NiMoL weld metals. *The 18th ASM Heat Treating Society Conference and Exposition.* Chicago, Ill.

10. Akselsen, O. M., Rorvik, G., Kvaale, P. E., and Van der Eijk, C. 2004. Microstructure-property relationships in HAZ of new 13% Cr martensitic stainless steel. *Welding Journal* 83(5): 160–167.

11. Lyttle, K. 1996. Metal cored wires: Where do they fit in your future? *Welding Journal* 74(10): 35–38.

12. Karlsson, L., Rigdal, S., Van den Broek, J., Goldschmitz, M., and Pedersen, R. 2002. Welding of supermartensitic stainless steels. Recent developments and application experience. *Svetsaren* No 2:15–22.

13. Zappa, S., Svoboda, H., Ramini de Rissone, M., Surian, E., and de Vedia, L. 2006. Effect of shielding gas on the supermartensitic stainless steel all weld metal properties. CONAMET/SAM 2006. Santiago de Chile, Chile.

14. ANSI/AWS A5.22-95, *Specification for Stainless Steel Electrodes for Flux Cored Arc Welding and Stainless Steel Flux Cored Rods for Gas Tungsten Arc Welding.* 1995. Miami, Fla.: American Welding Society.

15. ANSI B31.3-96, *Chemical Plant and Petroleum Refinery Piping.* 1996. New York, N.Y.: American National Standards Institute.

16. Bilmes, P. D., Llorente, C., Desimoni, J., and Mercader, R. 1997. Microstructure and properties of soft martensitic stainles steel weld metals. *2do Congresso Internacional de Tecnología Metalúrgica e de Materiais.* São Paulo, Brazil.

17. Lippold, J., and Alexandrov, B. 2004. Phase transformation during welding and post-weld heat treatment of a 12Cr-6.5Ni-2.5Mo supermartensitic stainless steel. *Stainless Steel World 2004.* Houston, Tex.

18. Bilmes, P. D., Llorente, C., Desimone, J., Mercader, R., and Solari, M. 1998. Microstructure and properties of 13% Cr - 4% NiMo martensitic stainless steel FCAW weld metals.. II Encuentro de Ingeniería de Materiales. La Habana, Cuba.

19. ASTM E562-99, *Standard Test Method for Determining Volume Fraction by Systematic Manual Point Count.* 1999. West Conshohocken, Pa.: ASTM International.

20. Cullity, B. D., and Stock, S. R. 2001. *Elements of X-Ray Diffraction.* New Jersey, Prentice-Hall. 3rd Edition.

21. ASTM E23-05, *Standard Test Methods for Notched Bar Impact Testing of Metallic Materials.* 2005. West Conshohocken, Pa.: ASTM International.

22. ASTM E8-04, *Standard Test Methods for Tension Testing of Metallic Materials.* 2004. West Conshohocken, Pa.: ASTM International.

23. Vaidya, V. 2002. Shielding gas mixtures for semiautomatic welds. *Welding Journal* 81(9): 43–48.

24. Stembacka, N., and Persson, K. A. 1989. Shielding gases for gas metal arc welding. *Welding Journal* 68(11): 41–47.

25. Gough, P. C., Farrar, J. C. M., and Zhang, Z. 1999. Welding consumables for supermartensitic stainless steels. *Supermartensitic Stainless Steel '99.* Brussels, Belgium.

26. Karlsson, L., Rigdal, S., Dhooge, A., Deleu, E., Goldschmitz, M., and Van den Broek, J. 2001. Mechanical properties and ageing response of supermartensitic weld metals. *Stainless Steel World 2001.* The Hague, The Netherlands.

27. Technical Sheet OK Tubrod. 2004. 15-55 ESAB.

28. Bilmes, P. D., Solari, M., and Llorente, C. L. 2001. Characteristics and effect of austenite resulting from tempering of 13Cr-NiMo martensitic steel weld metals. *Materials Characterization* 46: 285–296.

29. Karlsson, L., Rigdal, S., Dyberg, P., Van den Broek, J., and Goldschmitz, M. 2002. Submerged arc welding of supermartensitic stainless steel: Good as welded toughness — realistic or not? *Supermartensitic 2002.* Houston, Tex.

30. Karlsson, L., Rigdal, S., Bruins, W., and Goldschmitz, M. 1999. Efficient welding of supermartensitic stainless steels with matching composition consumables. *Stainless Steel Word 1999.* The Hague, The Netherlands.

31. Bilmes, P. D., Llorente, C. L., and Ipiña, J. P. 2000. Toughness and microstructure of 13Cr4NiMo high strength steel welds. *Journal of Materials Engineering and Performance* 9(6): 1–19.

32. Gooch, T. G., Woollin, P., and Haynes, A. G. 1999. Welding metallurgy of low carbon 13% chromium martensitic steels. *Supermartensitic Stainless Steel.* Brussels, Belgium.

33. Folkhard, H. 1988. *Welding Metallurgy of Stainless Steels.* Springer-Verlag Wien, New York.

34. Bilmes, P. D., Llorente, C. L., and Solari, M. 2000. Role of the retained austenite on the mechanical properties of 13Cr-4NiMo weld metals. *The 20th ASM Heat Treating Society.* St. Louis, Mo.

35. Bilmes, P. D., Llorente, C., Saire Huamán, L., Gassa, L. M., and Gervasi, C. A. 2006. Microstructure and pitting corrosion of 13CrNiMo weld metals. *Corrosion Science* 48: 3261–3270.

36. Marshall, A. W., and Farrar, J. C. M. 2001. Welding of ferritic and martensitic 11–14% Cr steels. *Welding in the World* 2001 Vol. 45 (5/6): 32–55.

37. Ramirez, J. E. 2007. Weldability evaluation of supermartensitic stainless steels. *Welding Journal* 86(5): 125-s to 134-s.

38. Bonnefois, B., Coudreuse, L., Toussaint, P., and Dufrane, J. J. 2002. Development in GMAW of new martensitic stainless steels. *Supermartensitic 2002.* Houston, Tex.

39. Bilmes, P. D., Llorente, C., and Solari, M. 1999. Effect of post weld heat treatment on 13%Cr4NiMo steel FCAW deposit. X Congreso Argentino de Soldadura — VI Congreso Iberoamericano de Soldadura. Buenos Aires, Argentina.